On applying the knock sensor for injector calibration

**Konrad Christ, Kristine Back, Thomas Kieweler, Uwe Kiencke
and Fernando Puente León**

Abstract

This article investigates the possibility of utilizing the standard knock sensor for an in situ injector calibration. The goal is to estimate the actual injection duration by means of the structure-borne sound emission during the injection process. Since the sound signals are highly nonstationary and contain various transients, a time–frequency analysis is applied. Based on the findings of the signal analysis, a method is presented for detecting the beginning and the end of injection by applying the theory of the change-point problem.

Introduction

The latest exhaust emission standards for internal combustion engines force carmakers and suppliers to develop cleaner and more fuel-efficient technologies. To face this challenge, modern gasoline engines are equipped with direct injection systems.[1,2] The precision of fuel metering is thereby a key issue for optimizing the combustion process and the exhaust emissions.

Due to manufacturing and component tolerances, the performance of different injectors for gasoline direct injection (GDI) varies considerably. Assembly and wear lead to further deviations and thus to imprecise fuel dosage. These discrepancies can be met by adapting the injection control. Therefore, a calibration system is required to improve the fuel injection throughout the entire service life.[3] At a constant fuel pressure, the injection process can mainly be characterized by the injector's opening duration. Hence, the goal of this article is to retrieve the relation between the injection duration and the supply control duration as it is done in Christ et al.[4]

The sound and vibration behavior is of great importance for fuel delivery systems. In terms of sound quality, the air-borne sound needs to be attenuated as much as possible. The corresponding structure-borne sound, on the other hand, can be used for monitoring the on-going contact-free process. The authors propose a method for an in situ calibration of GDI injectors based on an evaluation of the emitted structure-borne sound during the fuel injection process.

Figure 1 depicts the authors' idea of an in situ injector calibration.[4] The cylinder head and the entire engine block are excited by the vibration of the fuel injectors. The actual injection duration, that is, opening duration T_o of the fuel injector, is estimated out of the structure-borne sound signal $y(t)$ to give a feedback to the engine control unit (ECU). According to the estimation $T_{o, est}$, an adaptation of the supply control duration T_i can be performed in each operating point. In order to avoid higher costs and modifications, either of the injector or the cylinder head, the method proposed in this article is aimed at utilizing the knock sensors, which are conventionally mounted on the engine block of spark-ignition engines.[5]

The application of utilizing the knock sensor for injector calibration was already presented in Christ et al.[4] The authors showed a simple algorithm, which can determine the injector's opening and closing time to a certain control duration T_i. This approach requires

Institute of Industrial Information Technology, Karlsruhe Institute of Technology (KIT), Hertzstrasse 16, 76187 Karlsruhe, Germany

Corresponding author:
Konrad Christ, Institute of Industrial Information Technology, Karlsruhe Institute of Technology (KIT), 76187 Karlsruhe, Germany.
Email: konrad.christ@gmx.de
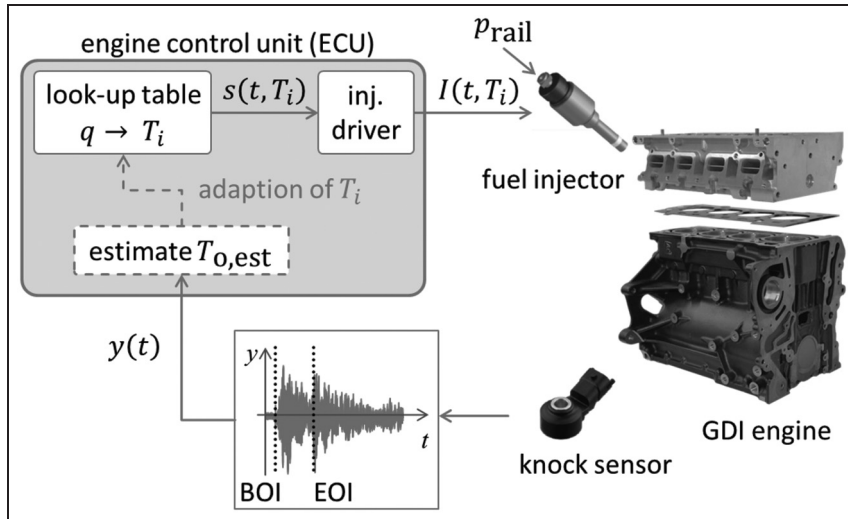
Figure 1. Calibration of GDI via structure borne sound.
BOI: beginning of injection; EOI: end of injection; GDI: gasoline direct injection.
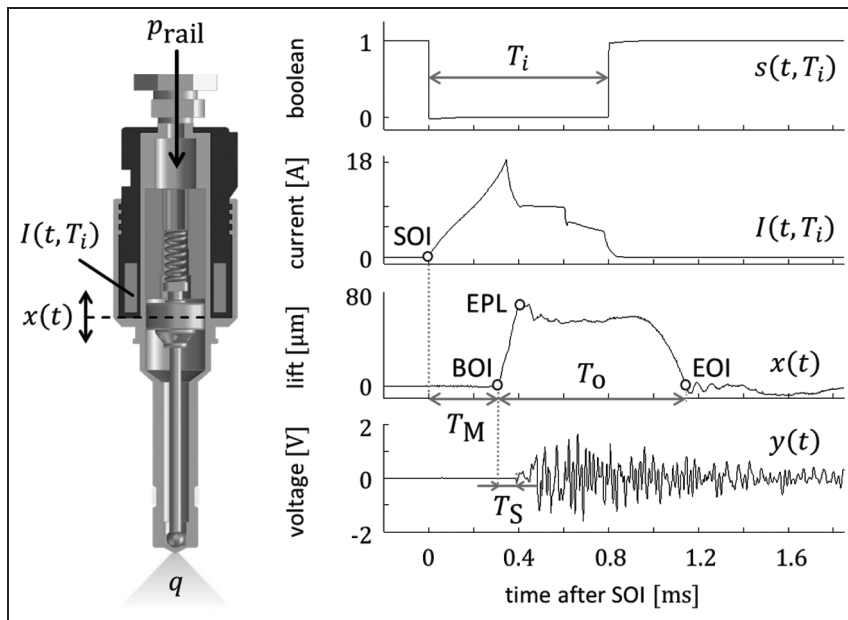
Figure 2. Structure and functionality of solenoid injector.
SOI: start of injection; BOI: beginning of injection.

a set of injection recordings and hence is not applicable to analyze single shots. However, the underlying document presents a new method, with which the injector's shot-to-shot variation of the injection duration and the fuel mass can be analyzed.

This article is structured as follows: A brief description of the injector and the fuel injection process are given in section "Fuel injector and fuel injection process." Since the aim of this report is the estimation of the actual injection duration, the structure-borne sound emissions need to be analyzed in detail. Therefore, the authors use an adapted time–frequency representation (TFR) based on the Wigner–Ville distribution (WVD). The derivation is given in section "Time–frequency signal analysis." In section "Structure-borne sound analysis," the TFR is applied to measurements of the emitted structure-borne sound during fuel injection. Based on the insights gained by the signal analysis, a method for estimating the actual injection duration is presented in section "Estimation of injection duration." In contrast to Christ et al.,[4] the estimation $T_{o,est}$ is performed on a single measurement of the structure-borne sound by applying the theory of change-point detection. The results are discussed in section "Results," and the conclusions are drawn in section "Conclusion."

Fuel injector and fuel injection process

The observed fuel injection valve is an inward opening solenoid-controlled injector, which is commonly deployed in modern GDI engines.[6] Figure 2 shows a schematic cross-sectional representation. The injector

basically consists of a pintle and a solenoid, which is powered by the current $I(t, T_i)$. The current is generated by the injector driver, which processes the control signal $s(t, T_i)$. The control signal is a low-active impulse of length T_i, which is the supply control duration. The start of injection (SOI) corresponds to the falling edge of $s(t, T_i)$ and thus stands for the start of the injector's activation. The pintle is lifted after a certain delay of magnetization T_M, and fuel is sprayed into the cylinder (beginning of injection (BOI)). Figure 2 also depicts the lift of the injector's pintle along with the control signal $s(t, T_i)$ and the corresponding injector current $I(t, T_i)$. The pintle lift is recorded by a laser vibrometer, as will be shown in section "Structure-borne sound analysis." If the injector's energization is long enough, the anchor hits the solenoid's core end of pintle lift (EPL). On deactivating the current, the magnetic field drops and the pintle shuts the nozzle, end of injection (EOI). The time span between BOI and EOI corresponds to the injection duration T_o.

During the injection process, the cylinder head is excited, which leads to structure-borne sound emissions on the cylinder head and the engine block. The lower part of Figure 2 depicts the emitted structure-borne sound, which will be examined in section "Structure-borne sound analysis." The BOI can be determined directly out of the signal amplitude $y(t)$. Due to the sound transmission time T_s, the instant of the BOI in $y(t)$ is delayed accordingly. The EOI, however, is superimposed on structure-borne sound waves of preceding events. Hence, its detection is not trivial in the time-domain signal. By having a closer look at the pintle lift, one can clearly see that the pintle oscillates with a certain frequency around $f = 15$ kHz after the EOI. This frequency can be assigned to the bouncing of the injector's pintle onto the nozzle and will be of major importance for the following considerations.

Time–frequency signal analysis

In this section, the methods for analyzing the knock sensor signals are presented. The goal of the signal analysis is to find out whether the EOI can be detected in the knock sensor signal. Therefore, an investigation of their frequency characteristics is of great interest. Since structure-borne sound signals of transient events are highly nonstationary, TFRs are applied to study their spectra as a function of time. The goal hereby is to obtain time–frequency spectra that allow a precise localization of events in both time and frequency.

Linear TFRs, such as the short-time Fourier transform (STFT) and the wavelet transform (WT), are widely used tools for time–frequency signal analysis. However, they suffer from the uncertainty principle, meaning that a high resolution in both time and frequency directions cannot be achieved simultaneously. Due to this, they have proved unsuitable for the task at hand. For this reason, quadratic TFRs based on the WVD are considered, which do not necessarily underlie the uncertainty principle.[7]

WVD

The WVD $W_{yy}(t,f)$ of a signal $y(t)$ represents the signal's energy density over time and frequency

$$E_y = \iint\limits_{\infty}^{\infty} W_{yy}(t,f)\,\mathrm{d}t\,\mathrm{d}f \tag{1}$$

Consider a two-dimensional correlation function of time and frequency shift, the so-called ambiguity function (AF) $A_{yy}(\nu, \tau)$ of $y(t)$

$$\begin{aligned}A_{yy}(\nu, \tau) &= \int_{\infty}^{\infty} y\left(t + \frac{\tau}{2}\right) y^*\left(t - \frac{\tau}{2}\right)\exp(\mathrm{j}2\pi\nu t)\mathrm{d}t \\ &= \mathcal{F}_\nu^{-1}\left\{y\left(t + \frac{\tau}{2}\right)y^*\left(t - \frac{\tau}{2}\right)\right\}\end{aligned} \tag{2}$$

where τ is the lag variable and ν is the Doppler variable. The WVD can be calculated as the Fourier transform of $A_{yy}(\nu, \tau)$ with respect to ν and τ

$$\begin{aligned}W_{yy}(t,f) &= \mathcal{F}_\tau\left\{\mathcal{F}_\nu\left\{A_{yy}(\nu, \tau)\right\}\right\} \\ &= \int_{\infty}^{\infty} y\left(t + \frac{\tau}{2}\right)y^*\left(t - \frac{\tau}{2}\right)\exp\left(-\mathrm{j}2\pi f\tau\right)\mathrm{d}\tau\end{aligned} \tag{3}$$

For a discrete time signal $y(n)$, $n = 0, \ldots, N - 1$, with the sampling frequency f_s, the discrete WVD $W_{yy}(n, k)$ is calculated as

$$\begin{aligned}W_{yy}(n, k) = 2 \cdot \sum_{m=-(N-1)}^{N-1} &y(n + m)y(n - m) \\ &\cdot \exp(-\mathrm{j}4\pi km/N)\end{aligned} \tag{4}$$

with the discrete frequency index $k = 0, \ldots, N - 1$, where $f = k \cdot f_s/N$.

Unlike the wavelet and STFTs, the WVD is not calculated by correlating the signal with families of time–frequency atoms. Thus, the time–frequency resolution of the WVD is not affected by the uncertainty principle. The WVD's practical use is limited; however, due to the fact that it is impaired by the formation of interference terms in case of nonstationary and multicomponent signals. Those cross terms can be attenuated by filtering the WVD, which, in turn, leads to leakage and therefore a lower resolution in the time–frequency plane. A good trade-off between resolution and interference is desired allowing a clear and easy signal analysis while meeting the requirements in accuracy. The authors propose applying a TFR of Cohen's[8] class, as will be discussed in the following section.

Smoothed Choi Williams distribution

TFRs of Cohen's class can be obtained by a multiplication of the AF with a low-pass kernel $\Phi(\nu, \tau)$ before applying the Fourier transform in equation (2)

$$\rho_{yy}(t,f) = \mathcal{F}_\tau\left\{\mathcal{F}_\nu\left\{A_{yy}(\nu, \tau) \cdot \Phi(\nu, \tau)\right\}\right\}$$
$$= \mathcal{F}_\tau\left\{y\left(t + \frac{\tau}{2}\right)y^*\left(t - \frac{\tau}{2}\right) \cdot K(t, \tau)\right\} \quad (5)$$

corresponding to a convolution with $K(t, \tau) = \mathcal{F}_\nu\{\Phi(\nu, \tau)\}$ in the time-lag domain.

The Choi–Williams distribution (CWD)[8,9] is a member of Cohen's class, with the kernel

$$\Phi_{\text{CW}}(\nu, \tau) = \exp\left(-\frac{\nu^2\tau^2}{\sigma}\right) \quad (6)$$

$$K_{\text{CW}}(t, \tau) = \frac{\sqrt{\pi\sigma}}{|\tau|} \cdot \exp\left(-\frac{\pi^2\sigma t^2}{\tau^2}\right) \quad (7)$$

The parameter σ controls the kernel width and therefore the trade-off between interference attenuation and keeping a fine resolution.

The authors propose an additional multiplication of K_{CW} with a Hamming window $g(t)$ in time direction and a Hann window $h(\tau)$ in lag direction for a further cross-term attenuation

$$K(t, \tau) = g(t) \cdot h(\tau) \cdot K_{\text{CW}}(t, \tau) \quad (8)$$

Following Boashash,[7] we calculate the discrete TFR as

$$\rho_{yy}(n, k) = 2 \sum_{m=-(N-1)}^{N-1} K(n, m)$$
$$*_n [y(n + m)y(n - m)] \exp(-j4\pi km/N) \quad (9)$$

with

$$K(n, m) = g(n) \cdot h(m) \cdot \frac{\sqrt{\pi\sigma}}{2|m|}\exp\left(-\frac{\pi^2\sigma n^2}{4m^2}\right) \quad (10)$$

The attenuation of the interference terms and the resolution of the TFR depend on the kernel width σ and the widths T_g and T_h of the windows $g(t)$ and $h(\tau)$. The choice of appropriate parameter values for the analysis of the knock sensor signals is discussed in the following section.

Choice of parameters

An adequate choice of the TFR's parameters is crucial for the analysis of the knock sensor signals. The time window in equation (10) corresponds to a Doppler window $G(\nu)$ in the ambiguity plane. This not only suppresses cross terms between frequency-shifted signal components but also causes a smearing of the TFR in time. The multiplication with the lag window $h(\tau)$ reduces interference in the time direction but lowers the resolution in frequency. For our purposes, we desire a high accuracy as well as suppressed interference in the

time direction while allowing some trade-offs in the frequency direction. Therefore, the width T_g of $g(t)$ must not be too long in order to keep the leakage in the time direction low. The width T_h of the lag window must be short enough to largely prohibit the formation of cross terms between time-shifted signal components. For analyzing the knock sensor signals, an appropriate width range of the time window is $T_g = 100, \ldots, 700\,\mu s$ and for the lag window $T_h = 120, \ldots, 200\,\mu s$.

For determining a good value for the kernel width σ, a quantitative performance measure for the TFR is utilized. The relevant aspects to consider thereby are the concentration of the TFR and the suppression of cross terms. First, the signal energy is normalized

$$E = \sum_n \sum_k \rho_{yy}(n, k) = 1 \quad (11)$$

Then, a criterion representing the concentration of the signal energy in the time–frequency domain is formulated according to[7]

$$M = \left(\sum_n \sum_k |\rho_{yy}(n, k)|^{1/2}\right)^2 \quad (12)$$

Small values of M indicate well-concentrated signal energy and thus a good compromise between resolution and interference reduction. The optimal value for σ can be obtained by minimizing equation (12). For the window lengths considered here and a sampling frequency of $f_s = 500\,kHz$, this yields $\sigma = 8\ldots 9$.

To demonstrate the superiority of the presented method, the resulting adapted TFR $\rho_{yy}(t, f)$ of the knock sensor signal is depicted in Figure 2 along with the corresponding STFT $S_y(t, f)$ and WVD $W_{yy}(t, f)$. While the STFT's precision is clearly insufficient for the task at hand, the WVD is so strongly affected by cross terms that no information can be gained from it. In contrast, the proposed version of the CWD allows a detailed examination of the knock sensor signals' time varying frequency content, as will be performed in the next section (Figure 3).

Structure-borne sound analysis

The aim of this article is the estimation of the actual opening duration of a fuel injector by processing the knock sensor signal. Before an adequate method can be presented, the structure-borne sound emissions during the injection process as well as the knock sensor signal itself need to be analyzed in detail. For that purpose, the TFR derived in the last section shall be used for evaluating the signals in the time–frequency domain. In the first part of this section, structure-borne sound signals recorded nearby the fuel injector are compared to measurements of the injector's pintle lift. In the second part, the knock sensor signal is investigated under real conditions in a custom four-cylinder GDI engine of type GM L850.
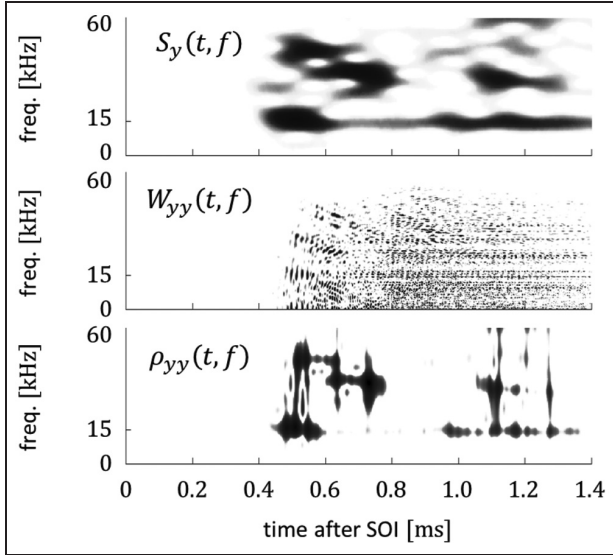
Figure 3. Structure borne sound emission during fuel injection. Comparison between different TFRs: STFT $S_y(t, f)$, WVD $W_{yy}(t, f)$ and the proposed TFR $\rho_{yy}(t, f)$. SOI: start of injection.

Figure 4. Test bench for structure borne sound analysis.

Structure-borne sound emission

As shown in Figure 2, the vibrating body of the fuel injector excites the cylinder head and structure-borne sound is emitted. By comparing the processed structure-borne sound signals with the measured pintle lift, a statement about the signal energy and the frequency content can be given for each single instant of time, especially for the BOI, the EPL and the EOI. For this, a standard knock sensor was mounted nearby the fuel injector on a special test bench, as can be seen in Figure 4. As a reference for the movement of the pintle, the pintle lift $x(t)$ was simultaneously acquired by a laser vibrometer during the injection process. Due to the small distance, the influence of the transfer function of the path between sensor and injector can be neglected in this case.

In the following, the knock sensor signals $y(t)$ are analyzed by applying the derived TFR and compared to the pintle lift $x(t)$. Figure 5 shows the measurements taken at the test bench for two operating points. In case of the left column, the supply control duration was chosen to be $T_i = 0.27$ ms at $p_{rail} = 10$ MPa. In this operating point, the pintle performs a ballistic movement and the anchor does not hit the solenoid's core, which means that the EPL does not take place. On the top, the injector current $I(t, T_i)$ is depicted. As explained in section "Fuel injector and fuel injection process," $I(t, T_i)$ is activated at the SOI and deactivated after the supply control duration T_i. The measured pintle lift $x(t)$ is plotted beneath and serves as a reference for the BOI and the EOI. After the EOI, a characteristic frequency of $f = 15$ kHz can clearly be seen in the progression of $x(t)$. This frequency is related to the bouncing of the injector's pintle, as already mentioned in section "Fuel
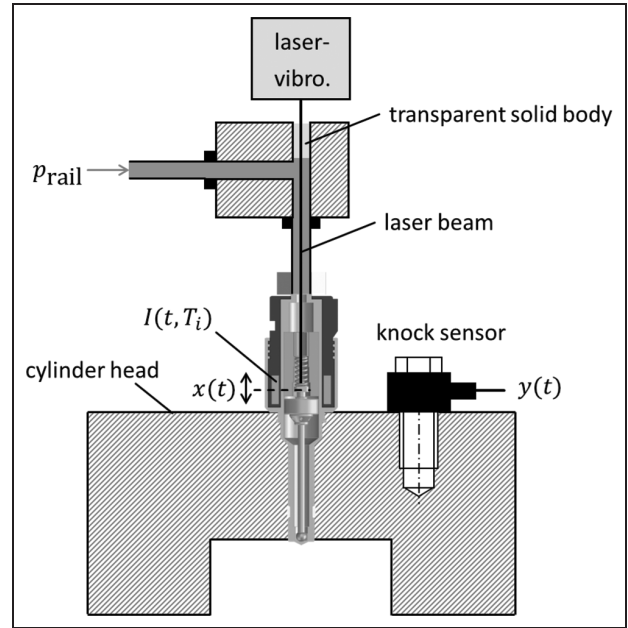
injector and fuel injection process." The BOI can easily be detected in the corresponding structure-borne sound signal $y(t)$. The sound running time is only around $T_s = 20$ µs for this experiment. The EOI, however, cannot be located within the time-domain signal $y(t)$. Applying the derived TFR reveals that the knock sensor signal contains the frequency $f = 15$ kHz, which indicates the EOI.

The same considerations for $T_i = 0.55$ ms are shown in Figure 5 in the right column. In this case, the injector performs a full pintle lift, so that the anchor hits the solenoid's core (EPL). Again, the BOI can easily be found in the time signal $y(t)$. The EOI, which is superimposed by structure-borne sound waves of preceding events, can be found in the TFR according to its characteristic frequency. Frequencies around $f = 20$ kHz are excited due to the EPL. Occurring frequencies $f = 40$ kHz are related to sensor resonances. The sensor's operating range is up to 30 kHz; thus, the sensor is suitable for detecting frequencies of interest around $f = 15$ kHz.

Knock sensor signal during engine run

The analysis in the last section showed that the BOI and EOI can be determined by placing a knock sensor nearby the injector. In this section, the standard knock sensor signals of a custom four-cylinder GDI engine of type GM L850 are examined. Every GDI engine of this type is equipped with two knock sensors knock sensor A (KSA) and knock sensor B (KSB) on the engine block. Sensor A is located between cylinders 1 and 2 and sensor B between cylinders 3 and 4. The recorded signals of one engine cycle, corresponding to two revolutions (720° crank angle (CA)) of the crankshaft, are depicted
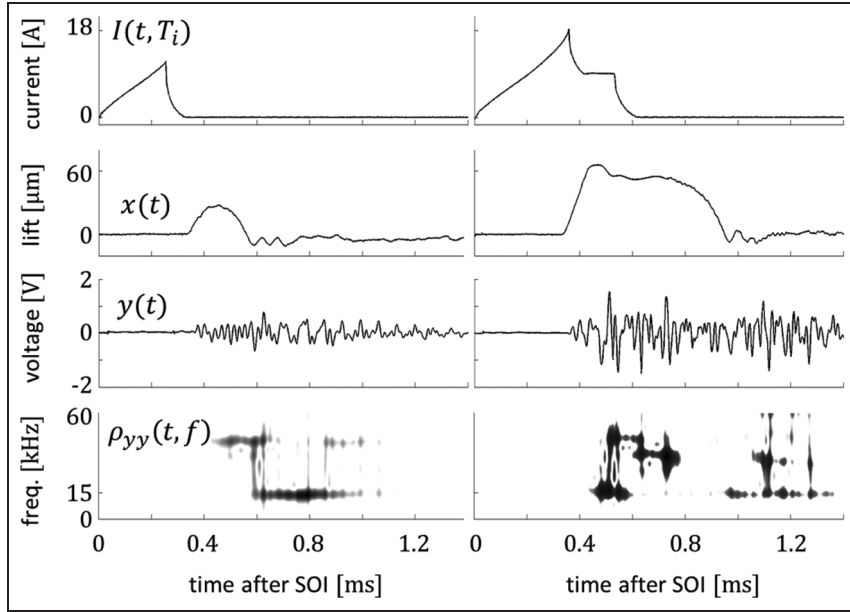
Figure 5. Pintle lift $x(t)$ and knock sensor signal $y(t)$ near the injector for $T_i = 0.27$ ms (left) and $T_i = 0.55$ ms (right) at $p_{rail} = 10$ MPa. SOI: start of injection.
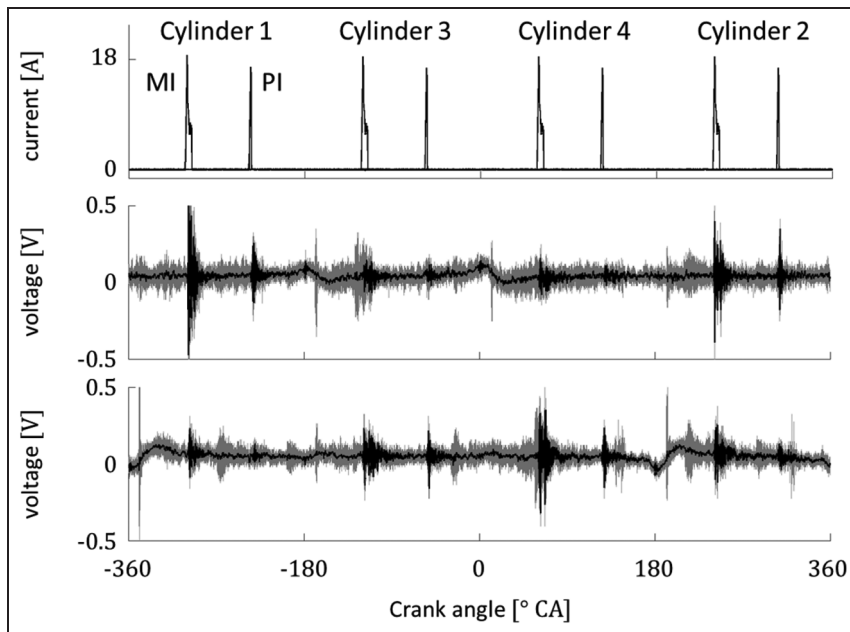
Figure 6. Knock sensor signals during engine run: 50 engine cycles of each $720°$ CA (gray), ensemble average (black), $n_{mot} = 1000$ r/min, $p_{rail} = 10$ MPa and ignition in cylinder 1 at $28.5°$ CA.
CA: crank angle; MI: main injection; PI: post injection.

in Figure 6. The control current of each cylinder is plotted in the top graph. The ignition sequence is 1-3-4-2, which means that an injection of cylinder 1 is followed by an injection of cylinder 3 with a delay of 180° CA. The knock sensor signals of 50 engine cycles are drawn in gray color depending on the CA. In each cycle, one main injection (MI) and one post injection (PI) per cylinder are carried out.

In spite of background noise, a detailed consideration of the injections of cylinder 1 reveals a highly systematic behavior, see Figure 7. The disturbances can be modeled as additive white Gaussian noise and attenuated by calculating the ensemble average of all measurements, which is depicted in black color. As previously described, the characteristic frequency $f = 15$ kHz can be observed in the time–frequency domain. Besides the fuel injection, the closing of the inlet and exhaust valves causes transients in the sensor signals. Their analysis shows, however, that these events do not exhibit a systematic behavior.
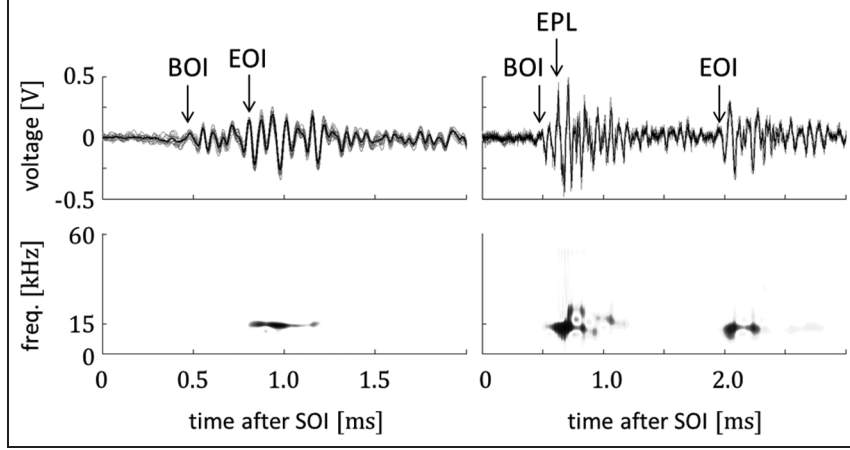
Figure 7. Post injection (PI) with $T_i = 0.28$ ms (left) and main injection (MI) with $T_i = 1.5$ ms (right) at $p_{rail} = 10$ MPa under real conditions (GM L850).

BOI: beginning of injection; EOI: end of injection; SOI: start of injection.

Estimation of injection duration

The structure-borne sound signals represent a sequence $y(n) \in \mathbb{R}$ in time, where $n = 0, \ldots, N - 1$. As shown in section "Structure-borne sound analysis," we clearly see several changes in the characteristics of the series. According to Lavielle,[10] the instants of the BOI and the EOI can be interpreted as change points. As has been shown, the BOI is related to a jump in the signal's amplitude. The EOI, however, is superimposed by structure-borne sound waves of preceding events and thus cannot be detected in the time-domain signal. The signal analysis revealed that the EOI excites frequencies around $f = 15$ kHz. This motivates the usage of a narrow frequency band around this frequency to detect the event.

This section outlines a detection strategy for the BOI and the EOI based on the theory of change-point detection as it is discussed in Basseville and Nikiforov[11] and Lavielle.[10,12] A brief introduction shall be given in the following section.

Change-point problem

The characteristics of the signal $y(n)$ change abruptly at some unknown change points n_s, where $s = 1, \ldots, S$ is the number of segments. The jumps are characterized by a parameter Θ that remains constant in the segments between two changes. In Lavielle,[12] different parameters Θ are discussed, such as the sequence's mean value, the variance or the spectral distribution.

According to Lavielle,[10] G is a function of the estimated parameter $\hat{\Theta}$ on each segment $1 \leqslant s \leqslant S$. Based on G, a contrast function

$$J = \frac{1}{N} \sum_{s=1}^{S} G(y(n_{s-1} + 1), \ldots, y(n_s)) \quad (13)$$

is formulated, which needs to be minimized to solve the change-point problem.

An effective implementation is realized by the stochastic approximation expectation maximization (SAEM) algorithm. The derivation and functionality of this algorithm shall not be part of this article. Details can be found in Basseville and Nikiforov[11] and Lavielle and coworkers.[12,13]

BOI detection

As the knock sensor signal is considered in a time window of accurate length after the SOI, the BOI is the first significant change in $y(n)$. The detection of the BOI is performed by choosing the signal's variance σ^2 as parameter Θ. As shown in Lavielle,[12] the Gaussian log-likelihood can be used to define

$$G(y(n_{s-1} + 1), \ldots, y(n_s)) = (n_s - n_{s-1}) \log(\hat{\sigma}^2) \quad (14)$$

for detecting the changes in the variance, where

$$\hat{\sigma}^2 = \frac{1}{n_s - n_{s-1}} \sum_{n=n_{s-1}+1}^{n_s} (y(n) - y)^2 \quad (15)$$

is the empirical variance of $y(n)$ in the segment s and y is the empirical mean value.

EOI detection

The results of section "Structure-borne sound analysis" clearly showed that the series $y(n)$ contains several changes in its spectral characteristics. As has been shown, the EOI excites certain frequencies. For detecting this event, the signal's energy density

$$E_y(n) = \sum_{k=k_1}^{k_2} \rho_{yy}(n, k) \quad (16)$$

is computed as a function of time in the discrete frequency band $[k_1, k_2]$, where $k_1 f_s / N \leqslant 15$ kHz $\leqslant k_2 f_s / N$ with sampling frequency f_s and $k = 0, \ldots, N - 1$.
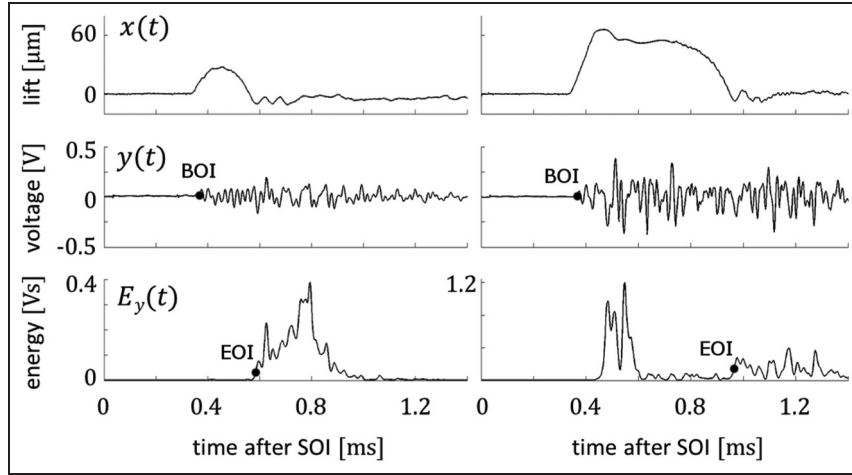
Figure 8. Energy density $E_y(n)$ of knock sensor signal $y(n)$ in frequency band around $f = 15\,\text{kHz}$.
BOI: beginning of injection; EOI: end of injection; SOI: start of injection.

This leads to Figure 8, where the energy density in the frequency band of interest is plotted along with the injector's pintle lift. At the instant of the EOI, the signal's energy density has a change point in the mean value. As suggested in Lavielle,[12] changes in the mean can be detected by applying

$$G(y(n_{s-1} + 1), \dots, y(n_s)) = \sum_{n=n_{s-1}+1}^{n_s} (y(n) - y)^2 \tag{17}$$

Lavielle and Ludena[14] discuss the change-point problem for spectral distributions. The suggested procedure is very similar to the proposed method in this article and yields nearly identical results.

Results

In order to assess the performance of the proposed method, the injection duration $T_{o,\text{est}}$ was estimated for different operating points T_i at a constant fuel pressure of $p_{\text{rail}} = 10\,\text{MPa}$ and compared to the reference $T_{o,\text{ref}}$ obtained by the laser vibrometer. The setup according to Figure 4 was used for this experiment since no direct reference for T_o is available during the engine run. Figure 9 shows the dependencies of $T_{o,\text{est}}$ and $T_{o,\text{ref}}$ from the supply control duration T_i. The discrepancies in the estimation can be attributed to difficulties in the detection of the EOI. For $T_i = 0.25, \dots, 0.3\,\text{ms}$, the pintle performs a ballistic movement and the EPL does not take place. In this interval, the behavior of different injectors varies considerably due to manufacturing dispersions and wear. Therefore, a calibration in this range is indispensable. Since the anchor does not hit the solenoid's core, only the abating structure-borne sound waves of the BOI interfere with the EOI. Hence, the EOI can be detected accurately. For $T_i = 0.35, \dots, 0.5\,\text{ms}$, the EOI occurs shortly after the EPL. For this reason, a reliable estimation cannot be
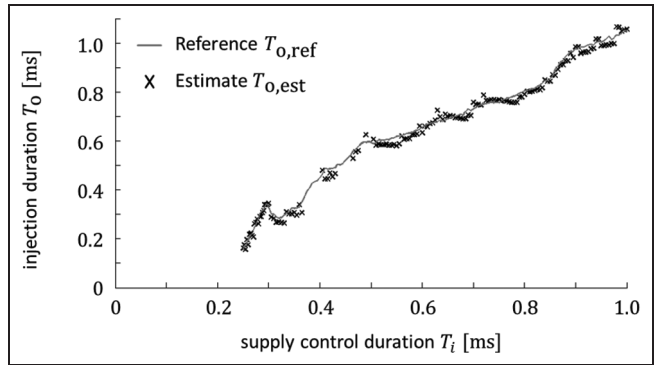
Figure 9. Estimation of actual injection duration $T_{o,\text{est}}$ for different T_i and a constant fuel pressure $p_{\text{rail}} = 10\,\text{MPa}$.

guaranteed in this interval. For $T_i > 0.5\,\text{ms}$, the EOI can be determined precisely.

Conclusion

This article showed that the standard knock sensors can be used for determining the actual injection duration of GDI systems. For this, an adapted TFR was used to analyze the structure-borne sound emissions during the injection process. On foundation of the resulting insights, the actual injection duration was estimated by applying the theory of change-point detection.

The derived method was used in an experimental setup to obtain a characteristic curve describing the relation between the supply control duration and the actual opening duration at a constant rail pressure. The performance of the method was evaluated by comparing the estimation results to laser vibrometer references yielding negligible deviations. Based on the estimated characteristic, an injector calibration can be performed by adapting the supply control duration accordingly. The integration and testing on an engine control unit (ECU) are yet to be performed.

References

1. Robert Bosch GmbH. *Gasoline engine management*. Chichester: Wiley Blackwell, 2006.
2. Robert Bosch GmbH. *Automotive handbook*. Chichester: Wiley Blackwell, 2007.
3. Hehle M, Willmann R, Remele J, Ziegler T and Schmidt G. In situ calibration high precision fuel injection for off highway engines. *ATZ* 2008; 4: 36 48.
4. Christ K, Back K, Jiqqir M, Kiencke U and Puente León F. Calibration of solenoid injectors for gasoline direct injection using the knock sensor. *MTZ Worldw* 2011; 4: 64 70.
5. Kiencke U and Nielsen L. *Automotive control systems*. Berlin: Springer, 2005.
6. Achleitner E, Koch A, Maier J and Marinai A. Solenoid controlled injectors for gasoline direct injection. *MTZ Worldwide* 2006; 67: 332 339.
7. Boashash B. *Time frequency signal analysis and processing*. Oxford: Elsevier Science, 2003.
8. Cohen L. Generalized phase space distribution functions. *J Math Phys* 1966; 7: 781ff.
9. Choi H and Williams W. Improved time frequency representation of multicomponent signals using exponential kernels. *IEEE T Acoust Speech* 2002; 37: 862 871.
10. Lavielle M. Optimal segmentation of random processes. *IEEE T Signal Proces* 1998; 46: 1365 1373.
11. Basseville M and Nikiforov I. *Detection of abrupt changes: theory and application*. New Jersey: Prentice Hall, 1993.
12. Lavielle M. Using penalized contrasts for the change point problem. *J Signal Process* 2005; 85: 1501 1510.
13. Delyon B, Lavielle M and Moulines E. Convergence of a stochastic approximation version of the EM algorithm. *Ann Stat* 1999; 27: 94 128.
14. Lavielle M and Ludena C. The multiple change points problem for the spectral distribution. *Bernoulli* 2000; 6: 845 869.

Appendix I
Notation

f_s	sampling frequency (kHz)
k	frequency index (–)
n	time index (–)
N	signal length (–)
p_{rail}	fuel pressure (MPa)
s	segment number (–)
T_i	supply control duration (ms)
T_o	injection duration (ms)
$x(t)$	pintle lift (μm)
$y(t)$	knock sensor signal (V)
ν	Doppler variable (Hz)
σ	kernel width (–)
σ_s^2	variance in segment s (V^2)
τ	lag variable (μs)

Repository KITopen

Dies ist ein Postprint/begutachtetes Manuskript.

Empfohlene Zitierung:

Christ, K.; Back, K.; Kieweler, T.; Kiencke, U.; Puente León, F.
On applying the knock sensor for injector calibration.
2014. International journal of engine research, 15.
doi:10.5445/IR/1000041139

Zitierung der Originalveröffentlichung:

Christ, K.; Back, K.; Kieweler, T.; Kiencke, U.; Puente León, F.
On applying the knock sensor for injector calibration.
2014. International journal of engine research, 15 (5), 597–605.
doi:10.1177/1468087413500059